1-1-1978

Experimental study of the propagation of long-wavelength disturbances through turbulent plow in tubes.

Robert Edwin Linney

EXPERIMENTAL STUDY OF THE PROPAGATION OF LONG-WAVELENGTH DISTURBANCES THROUGH TURBULENT FLOW IN TUBES

by

Robert Edwin Linney

A Thesis

Presented to the Graduate Committee

of Lehigh University

in Candidacy for the Degree of

Master of Science

in

Mechanical Engineering

Lehigh University

1978

CERTIFICATE OF APPROVAL

This thesis is accepted and approved in partial fulfillment of the requirements for the degree of Master of Science.

5 May 1978

(date)

Professor in Charge

Chairperson of Department

ACKNOWLEDGMENTS

I extend my sincere thanks and appreciation to Professor Forbes T. Brown, whose knowledge and advice made this project possible.

Special thanks is given to the department's technical staff for the contribution of their skill and experience.

TABLE OF CONTENTS

LIST OF FIGURES

ABSTRACT

Measurements of the phase velocity and attenuation factor for the propagation of long-wavelength sinusoidal perturbations through turbulent flow in tubes are reported. The frequency band of interest was between the band for which a quasi-steady-flow model applies and the band for which a constant or frozen eddy-viscosity model applies. The results indicate a relatively smooth transition between the two models. It is hoped these results will help improve analytical models of nonequilibrium turbulent boundary layers.

The principal test section comprised a tube, potted in concrete, sixty-one meters long and 6.23 mm in inner diameter, coiled in a helix with a diameter of 3.05 meters. The fluid as degassed water, the steady component of flow was impressed by compressed air in a tank, the perturbations were impressed by a motor-driven adjustable piston-cylinder assembly, and the measurements were made with small semiconductor strain-gage pressure transducers.

An earlier similar study which motivated the work suggested highly anomalous results tentatively identified as a resonance phenomenon associated with the excited non-

equilibrium turbulence. This result is not corroborated, and since the present data much more nearly corresponds to expectations based on current knowledge it is concluded that the earlier results are incorrect, possibly because of a faulty transducer mounting.

INTRODUCTION

The original objective of this experimental study was to verify and extend earlier results from which two pronounced absorption bands for oscillatory wave perturbations superimposed on a mean turbulent tube flow were inferred (Fig. 10 and 11) [2]. The frequency band of interest consisted of the transition band between which a quasi-steady-flow model and an eddy-viscosity model appeared to apply.

The original study, conducted at M.I.T., used a helically coiled test section with a diameter ratio of 384. In addition to the two sharp absorption bands the data appeared to show variations in the phase velocity up to 18% greater than the nominal acoustic speed. This behavior was consistent with the attenuation data if a resonance model was postulated. It was thought such a resonant model could be related to the deterministic sequence of events associated with the production of turbulent eddies in a boundary layer. This behavior occured only for turbulent flows and in the transition band. The data corroborated the low frequency or constant I-R-C model for dimensionless frequency $\Omega < 200$ and the high frequency model for $\Omega > 1200$ [1].

The present study started with a straight test section; the preliminary results (not given quantitatively herein) failed to confirm the existence of the absorption bands and anomalous phase velocity behavior. Next, a coiled test section with a diameter ratio of 102 was constructed and tested, since one hypothesis was based on the effects of secondary flow due to curvature. This too failed to indicate the anomalous results. Finally, the third apparatus which is the subject of this thesis was built and tested.

This apparatus had a diameter ratio of 408. This size was chosen to be similar to the M.I.T. test section in hope of observing a resonance phenomenon. The experimental results, as shown in Figures 8 and 9, again showed no such phenomenon, however. The attenuation data suggests, rather, a relatively smooth transition between the constant I-R-C model at low frequencies and the higher frequency eddy-viscosity model. An unexplained overshoot of the phase velocity peaked to 3% above the nominal acoustic speed, but this small anomaly was not associated with any evident resonance behavior.

EXPERIMENTAL CONCEPTS

The test section is basically a long cylindrical tube with a submerged open end, a sinusoidal oscillator at the opposite end and a mean fluid flow, as shown in Fig. 1. The generated waves propagate downstream, reflect, and return upstream. The experimental goal is the determination of the phase velocity and attenuation of the waves as they propagate through the mean turbulent flow. The forward and reverse waves exist simultaneously, so only their superposition can be measured at a point along the line.

The experimental concept used to deduce the behavior of these waves was developed by Brown, et. al. [2]. It involves the use of two pressure transducers, and a known, constant, and pressure as shown in Fig. 2. Assuming for the moment that the mean velocity has no effect, the measurable pressures at these three equidistant points can be expressed in terms of the pressures of the forward and reverse waves, p_1 and p_2, respectively.

$$p(-L) = p_1 e^{(jk+\alpha)L} + p_2 e^{-(jk+\alpha)L}$$

$$p(0) = p_1 + p_2$$

$$p(L) = p_1 e^{-(jk+\alpha)L} + p_2 e^{(jk+\alpha)}$$

Here κ is the wave number (which equals $\frac{\omega}{V_p}$ in which V_p is the phase velocity) and α is the attenuation factor. The amplitudes of the waves at 0 are the magnitudes of the complex numbers p_1 and p_2 , and the phase angles of the waves are represented by the phase angles of p_1 and p_2 . The magnitude and phase angle of the complex ratio

$$\frac{p(-L)+p(L)}{2p(0)} = \cosh\left[(jk+\alpha)L\right] = \cosh\alpha L \cos kL + j\sinh\alpha L \sin kL$$

can be determined experimentally. The magnitude and phase angle of this ratio are, respectively,

$$M = \left|\frac{p(-L)+p(L)}{2p(0)}\right| = \sqrt{\sinh^2\alpha L + \cos^2\alpha L}$$

$$\Phi = \angle\frac{p(-L)+p(L)}{2p(0)} = \tan^{-1}\left[\tanh\alpha L \tan kL\right]$$

These two equations can be solved for the desired unknowns, α and V_p .

$$\alpha = L^{-1}\ln\left(m + \sqrt{m^2+1}\right)$$

$$m = \sqrt{\frac{M^2-1}{2} + \sqrt{\left(\frac{M^2-1}{2}\right) + M^2\sin^2\Phi}}$$

$$V_p = \frac{\omega}{L^{-1}\tan^{-1}\left[\frac{\tan\Phi}{\tanh\alpha L}\right]}$$

The only effect of the Doppler bias is assumed to be an increase in the velocity of the downstream traveling wave and a decrease in the velocity of the upstream traveling wave. The error introduced by neglecting the mean velocity can be corrected approximately by increasing and decreasing the actual phase angle reported at $-L$ and L, respectively, by the angle ϵkL, where ϵ is the ratio of the mean bias velocity to the nominal phase velocity. This correction factor can be accurately determined and showed good agreement with the known data. A constant pressure correction was added to $p(-L)$ and $p(0)$ to account for static head due to their different elevations.

The analytical basis of the experimental model assumes a linear distributed system with one space dimension and time as its state variables. This framework requires two assumptions, the first of which is that the system is second order in the space dimension and thus can be represented by a two dimensional state vector. Higher order models have been shown to degenerate to a second order model and checks on known data confirm the validity of the simpler model.

The second assumption is that, aside from the Doppler bias, the waves propagate upstream with the same velocity and attenuation as they propagate downstream. This means that the system is symmetric except for the convective Doppler bias.

EXPERIMENTAL APPARATUS

A schematic of the basic experimental apparatus is shown in Fig. 1. The test section used was a 60.96m (200ft.) long, 3.048m diameter helical coil of 6.23mm I.D. thick wall tubing. The tubing was carefully rolled to the desired curvature, using a specially designed three-point-bending jig. The rims of the rollers were machined to conform to the cross section of the tubing. The tubing was bent continuously and there was little uneven deformation.

The supports for the helix were ten equally spaced 2×4's with protruding screw hooks spaced 25.4mm apart (see Fig. 4). The tubing was wired to the hooks and checked for trueness with a large radius gage. After successful steady-flow pressure-drop tests were conducted, the entire coil was potted in concrete to reduce energy losses through the tube walls.

The transducer blocks served two purposes, the first of which was to provide non-obtrusive pressure taps and the second of which was the smooth joining of the four 15.24m segments of the test section. The transducer blocks were designed to permit the complete purging of any air pockets. The presence of even a minute air bubble can give erroneous data. This point cannot be overemphasized. The compliance of the air causes unacceptable flow through the 1.59mm tap hole, affecting both the magnitude and phase angle of the measurement and possibly excessively affecting the wave propagation itself. The transducer holes were at 45° from the vertical and had a groove cut at a right angle to the threads, as shown in Fig. 5. This design helped remove air entrained in the transducer threads by providing a channel of low flow resistance to facilitate bleeding under pressure. The exterior openings of the threaded transducer ports were kept submerged at all times to prevent possible re-infiltration of air.

The exit end of the test line, as shown in Fig. 3, was submerged in a water-filled cylinder. The data reduction scheme assumes constant pressure at a point slightly downstream of the free end, to account for its effective acoustic length. According to [3] this is 0.307 of a diameter. During laminar runs, the Plexiglas cylinder was closed and pressurized to approximately one atmosphere to assure positive pressures and to prevent cavitation at the positive displacement oscillator. An inverted beaker with a minimum of 300cm of trapped air provided a compliance and a needle valve controlled the outlet flow rate. During turbulent runs the pressures were large enough to prevent cavitation, so the top of the cylinder was removed and the water overflowed at a constant level.

Three-quarters of a circumference of the helix was used as flow development length upstream of the first transducer. This length was in addition to the 60.96m test line.

Filtered deionized water, stored in a 0.28m stainless steel pressure vessel, was the working fluid. Deionization of the water seemed to give better calibrations and more repeatable data. Between runs, a 66cm of Hg vacuum was drawn above the free surface for a 24 hour period to degas the water. During runs, the vessel was pressurized with regulated clean air. This provided a noiseless driving force to propell the water at a desired rate.

Sinusoidal excitations were generated by a positive displacement driver shown schematically in Figure 1. A speed controlled D.C. motor, through a set of gears and timing belt, drove a variable stroke scotch yoke (12.7 to 102mm range). Identical opposing piston-cylinder sets were attached to the yoke. One cylinder was connected to a branch of the supply line upstream of the test section. The opposing cylinder was pressurized with regulated air with sufficient pressure to offset the time-averaged force from the water piston.

Figures 6 and 7 show the details of the different piston sets used. Both cylinders were made from a solid brass bar, bored and sleeved with extruded tubing. The pistons were tipped with leather seals. Leather with its low Poisson's Ratio, provides a relatively constant sliding frictional force under a varying pressure. Other piston designs were tried, but none sealed as well or ran as smoothly.

With the two piston sets and the variable stroke driver, volume displacements ranging from 0.10 to 7.24 cm^3 could be achieved at the oscillator. A series impedance to the perturbations is needed upstream of the oscillator to achieve a substantial pressure oscillation. This was achieved by a coil of small diameter tubing connected in parallel with a needle valve (Fig. 1). This coil provided a linear flow resistance approximating that of the test section.

A Digital Equipment Corporation, model PDP-8 mini-computer with 10-bit A/D converter, multiplexer programmable quartz clock, teletype and point-plot video display was used to collect, store and reduce the data. Kulite model XTMS-1-190-100 semiconductor pressure transducers were located at the beginning and the middle of the test line, as indicated in Figure 2. Signals from the transducer amplifiers were transmitted through low-noise shielded cables to sets of calibrated Honeywell model 122-1 D.C. linear amplifiers. The amplifiers permitted the signal amplitudes to be attenuated, amplified and offset. This allowed the voltage inputs to the mini-computer to be within the ± 1 volt range, which was converted to 10-bit numbers. A dual-trace oscilliscope monitored the inputs to the computor, aiding the adjustments of the amplifier gain and offset, and permitting judgement of the signal quality.

Steady-flow friction factor test results are tabulated below and compare satisfactorily to those of Moody [4], if a correction for the additional losses due to the twin-eddy secondary flow is added [5].

Reynolds number	5090	7200	11300
Friction factor data from Moody	.0370	.0339	.0275
Measured friction factor for test line	.0402	.0379	.0316
From White [6]	.0382	.0351	.0286
From Ito [7]	.0374	.0345	.0309

EXPERIMENTAL PROCEDURE

To employ the experimental concepts, the pressure ratio between the three equidistant points must be known. Since the two transducers and the static head above the exit were all referenced to the ambient pressure, it was unnecessary to know their absolute pressures. Only the pressure ratio between the two transducers must be known to determine the phase velocity and attenuation factor.

One technique for calibrating the transducer sensitivity ratio would be to perform a static calibration with both transducers in the same location. In addition to obvious problems associated with a remote calibration, this procedure allows no checks on correction factors employed or any of the system dynamics. Instead, a dynamic laminar calibration was performed using the turbulent data acquisition procedure with only the mean flow bias correction changed. Without the randomness and viscous layers of turbulent flow, laminar data is relatively easy to obtain and shows consistant agreement with established theory [1,2].

Prior to each data run, the vacuum over the degassed water was released and the vessel was pressurized to approximately two atmospheres with clean compressed air. All valves and plumbing upstream of the test section were flushed through the recirculation line (Fig. 1). After this flushing, the recirculation valve was closed and the ball valve to the test line was opened. The test section was then flushed with the newly degassed water. Only after this were the transducer locations bled. The purging groove in the threaded ports eliminated the need to remove the transducers. A Plexiglas model showed visually that it was only necessary to unscrew the transducer a few turns to remove the entrained air.

Following flushing procedures, the flow was stopped and the cover was clamped over the end section. An inverted beaker was used, as shown in Figure 3, to assure sufficient compliance for the pressure in the end section to have negligible fluctuations.

Valves to the impedence coil were then opened and the flow rate was regulated by the needle valve at the end section. The fluid temperature and flow rate were checked. Temperatures ranged from 16°-24°C and the calibration Reynolds number was 1000.

The scotch yoke driver was started after the proper piston, stroke and gearing were chosen. Low frequencies were used for laminar calibration because the sensitivities of the small phase angles made it easier to ascertain the quality of calibration. The stroke and piston combinations were generally selected to give the largest signal to noise ratio before piston cavitation occurred. The resulting velocity variations were less than roughly 12% of the mean flow velocity during turbulent runs.

The signal amplifier gains and offsets were adjusted, and the proper Reynolds number, temperature, nominal wave velocity, amplifier ratio and clock code were typed into the computer.

The trigger signal from the driver would trip the Schmidt trigger in the A/D converter which was connected to the programmable clock. The period of oscillation and the corresponding non-dimensional frequency, Ω, were printed out and checked for repeatability.

The data program would collect, store, and cycle average each 97-point digital sweep for a selected number of cycles (usually 30-50 cycles per printout). The computer did not read both channels simultaineously; a 54 μsec time lag correction was added to the second channel. The program also performed a fast Fourier transform on the averaged data to quantitize their sinusoidal quality. A point plot of both signals was displayed on the video screen before and after the data sweeps were taken. Most noise and harmonics coupled with the data frequency would show up on the display. The computer printout included the magnitude ratio, phase angle, and their corresponding phase velocity and attenuation factor.

Several laminar data runs were repeated at different frequencies to verify the system calibration. The acceptable calibration limits were $\pm$ 0.1% of the magnitude ratio and $\pm .05^\circ$ of phase angle. These tolerances were determined by the functional limits of the equipment and not by their desirability.

Following successful calibration, the cover and valve were removed from the end section so there was free runoff. The pressure in the blow tank was increased to 6 atmospheres and the flow rate was regulated to Re = 10,000 by cracking the upstream needle valve. Mass flow rate and temperatures were checked and entered into the computor.

Turbulent data was taken similarly to the calibration runs, although different problems existed. It was discovered that there was cross talk of as many as three bits between the channels if the signals crossed one another. The solution employed was to adjust the biases and gains to preclude signal crossing. This was not a limitation for small phase angles but, when the signals were out of phase or very noisy, the 10-bit range of the computor inputs was effectively reduced by one bit. The reduction of usable bits was partly compensated for by increasing the number of sweeps averaged, and was deemed more acceptable than a deterministic bias effect from the cross talk.

A final laminar run was performed immediately after the turbulent data was taken to check the acceptability and repeatability of the first calibration.

RESULTS AND DISCUSSION

The data for the attenuation factor and phase velocity for laminar and turbulent flows are shown in Figures 8 and 9. The laminar data shows excellent agreement with established theory over the entire frequency range. The turbulent results show no pronounced absorption bands or drastic phase velocity changes as observed with the previous apparatus (Fig. 10 and 11). The attenuation data infers a relatively smooth transition band while the normalized phase velocity shows an unexplained peak of 3% above the nominal acoustic speed.

Each data point plotted represents the mean of several printouts of cycle-averaged data at the same frequency. The individual printouts were the average of 30 to 50 sweeps, so the plotted points represent a minimum of 100 cycles each. The data was repeatable from day to day and showed no significant variation due to amplitude or piston changes.

The error bounds above and below the attenuation data for turbulent flow (shown in dashed lines) represents the combined errors of the data randomness and calibration inaccuracy. Standard deviations were calculated for the printouts of the individual repeated frequencies. The computer program was capable of calculating attenuation and phase velocity sensitivities to changes in the magnitude ratio and phase angle. These sensitivity ratios were multiplied by the allowable calibration range to give an approximate standard deviation due to equipment errors. These deviations were combined, appropriately, multiplied by 2, and plotted to represent two-standard-deviation bounds. No bounds are shown for the normalized phase velocity because the combined two-standard-deviation was always smaller than 0.8%. The logic behind the M.I.T. results appears to be sound, but the results themselves are not corroborated. According to Professor F.T. Brown, the only possible flaw he can detect in that work is the failure to check independently for error in the readings of the downstream transducer used (one out of three transducers) in that study. The transducer mounting was not as carefully constructed as in the present study, and a burr may have upset the flow. The resulting pressure disturbance would have had to exceed considerably the total perturbations in dynamic head, and this possibility had been discounted. Such unexpectedly large perturbations were indeed observed, however in a (different) early version of a transducer mount used in the present study. Unfortunately, the M.I.T. apparatus no longer exists so an autopsy is impossible.

Since the present results agree with expectations and known theory much better than the M.I.T. results, they are expected to be essentially correct.

The results should be useful in improving upon existing models for turbulent boundary layers. In particular they should aid in the determination of the primary time constant in the persistence of eddy viscosity.

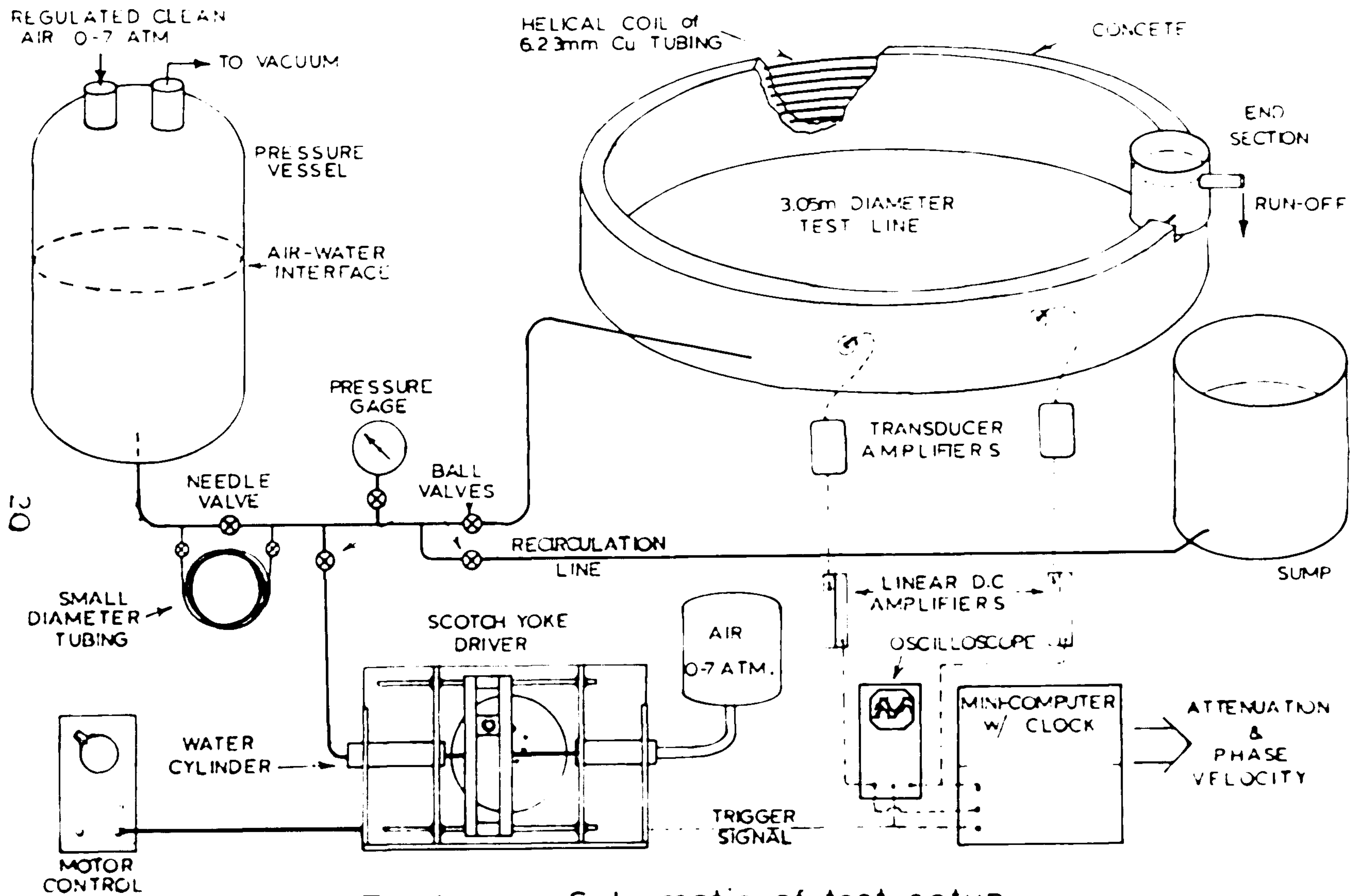

Fig. 1 Schematic of test setup

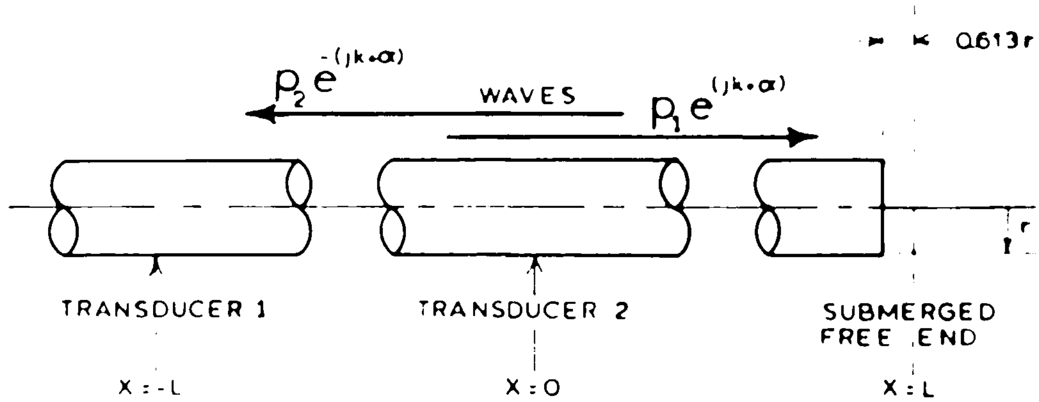

Fig. 2 Representation of test line

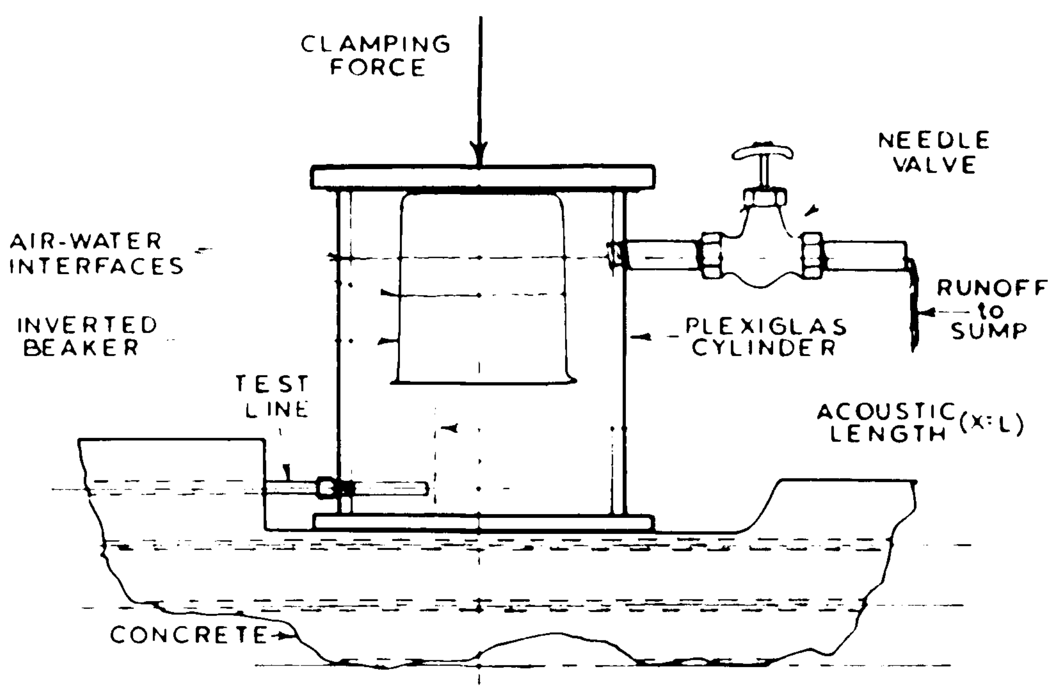

Fig. 3 Details of end section

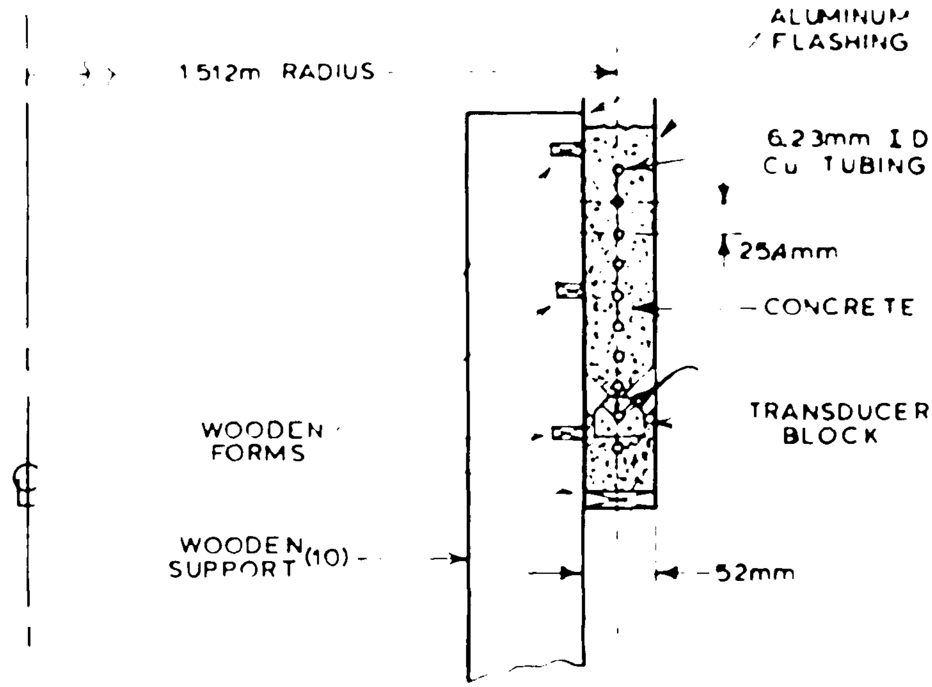

Fig. 4 Construction details

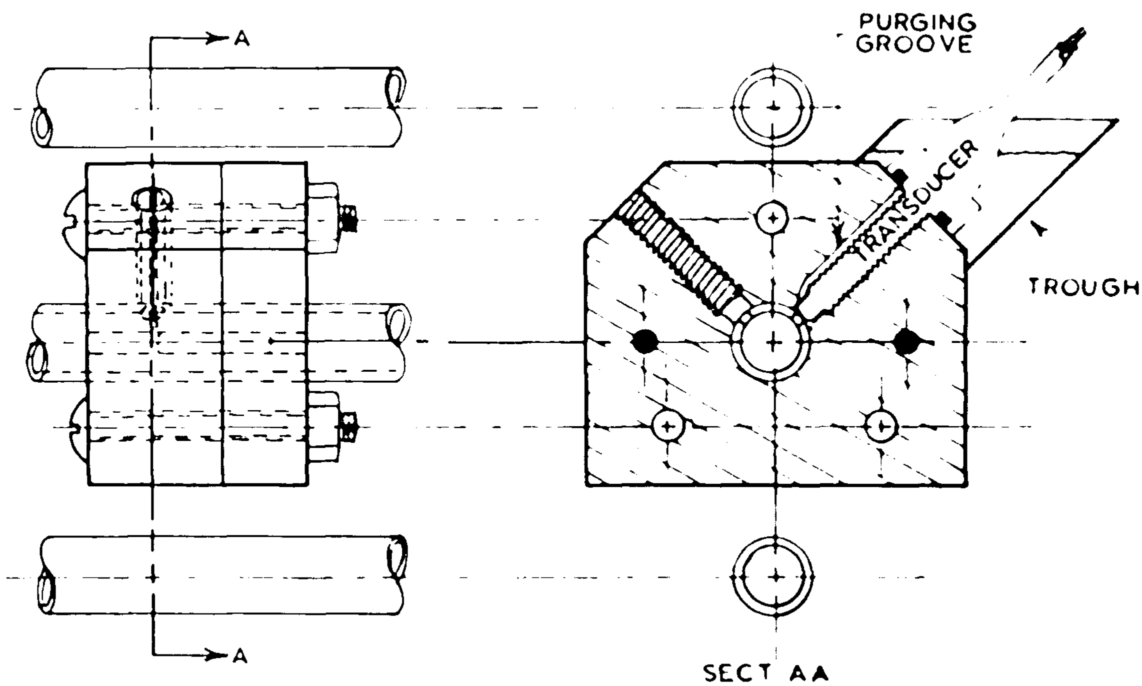

Fig. 5 Transducer block

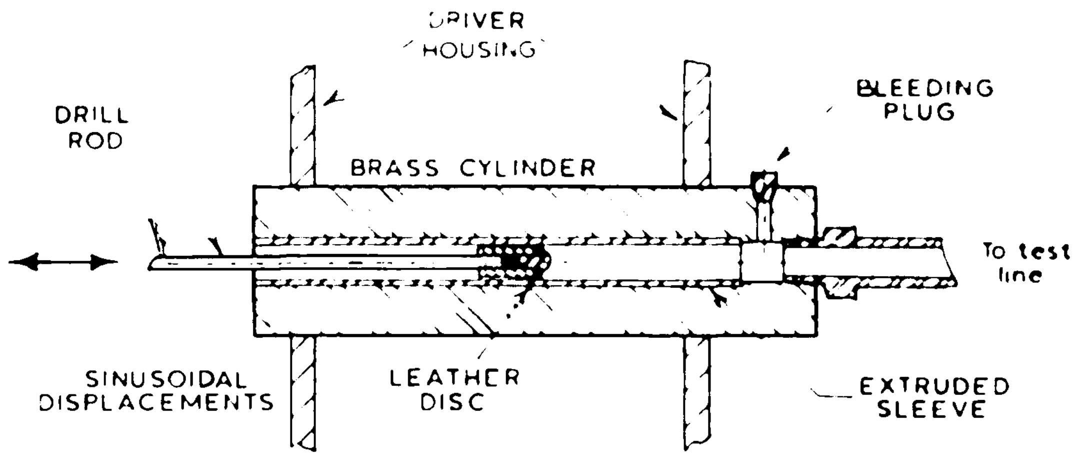

Fig. 6 Details of 9.53mm piston-cylinder

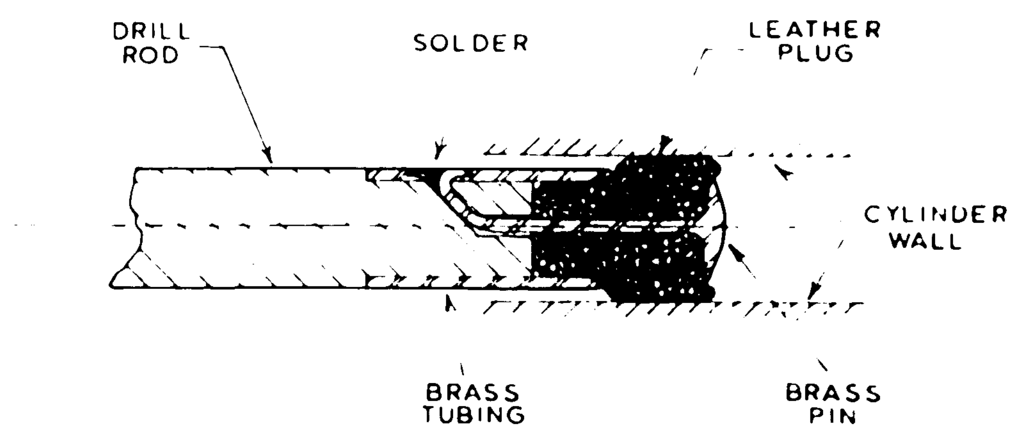

Fig. 7 Details of 3.18mm piston

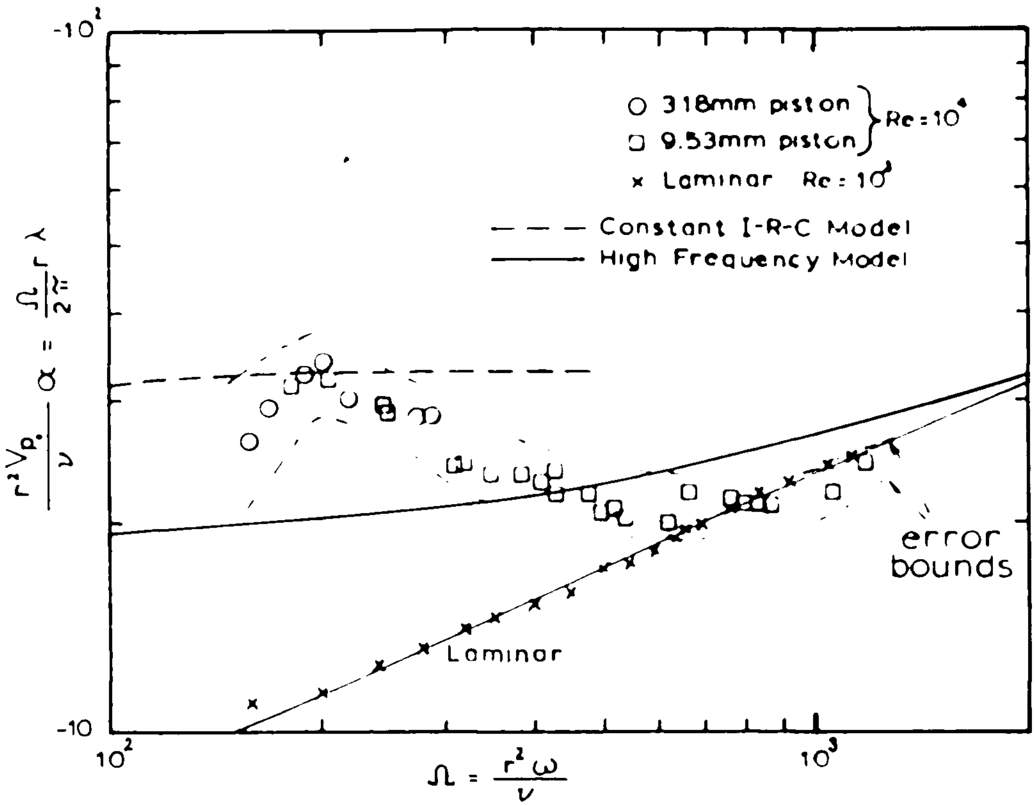

○ 318mm piston
□ 9.53mm piston
Re = 10⁴
× Laminar Re = 10³
Constant I-R-C Model
High Frequency Model
error bounds
Laminar
-10²
-10
10²
10³

Fig 8

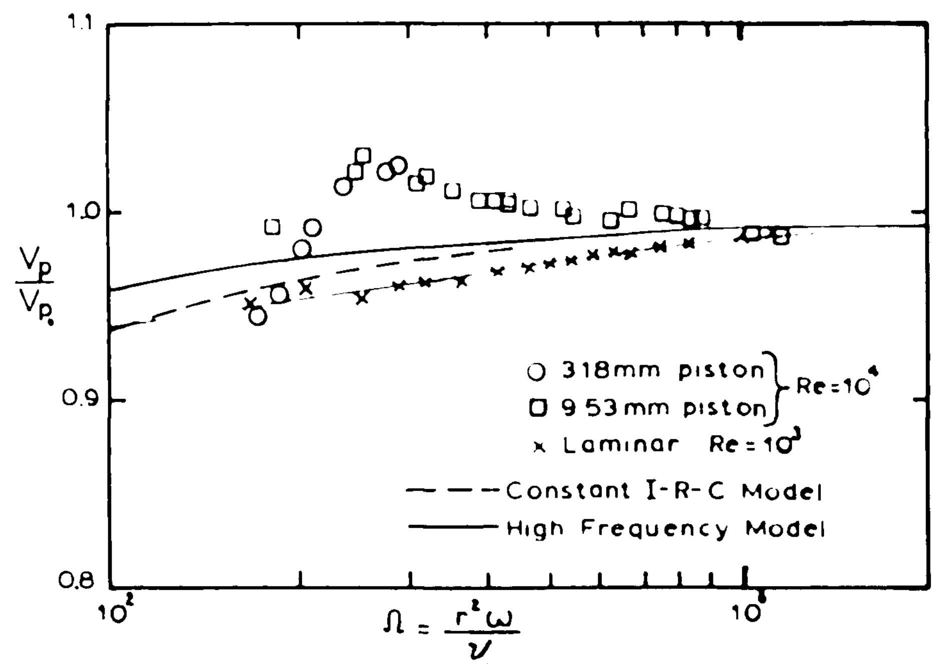

1.1
1.0
0.9
0.8
10²
10³
○ 318mm piston
□ 9.53mm piston
Re=10⁴
× Laminar Re=10³
Constant I-R-C Model
High Frequency Model

Fig. 9

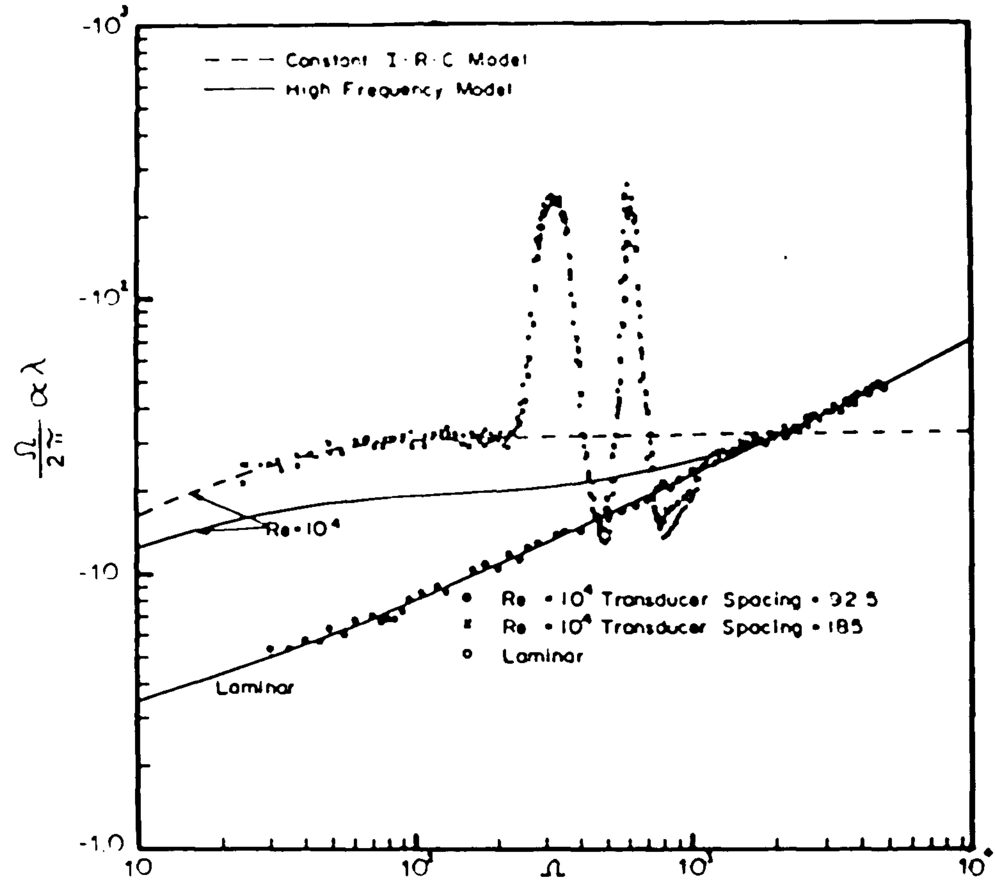

Constant I·R·C Model
High Frequency Model
Re = 10^4
Re = 10^4 Transducer Spacing = 92.5
Re = 10^4 Transducer Spacing = 185
Laminar
Laminar
$\frac{\Omega}{2\pi}\alpha\lambda$
Ω

Fig. 10

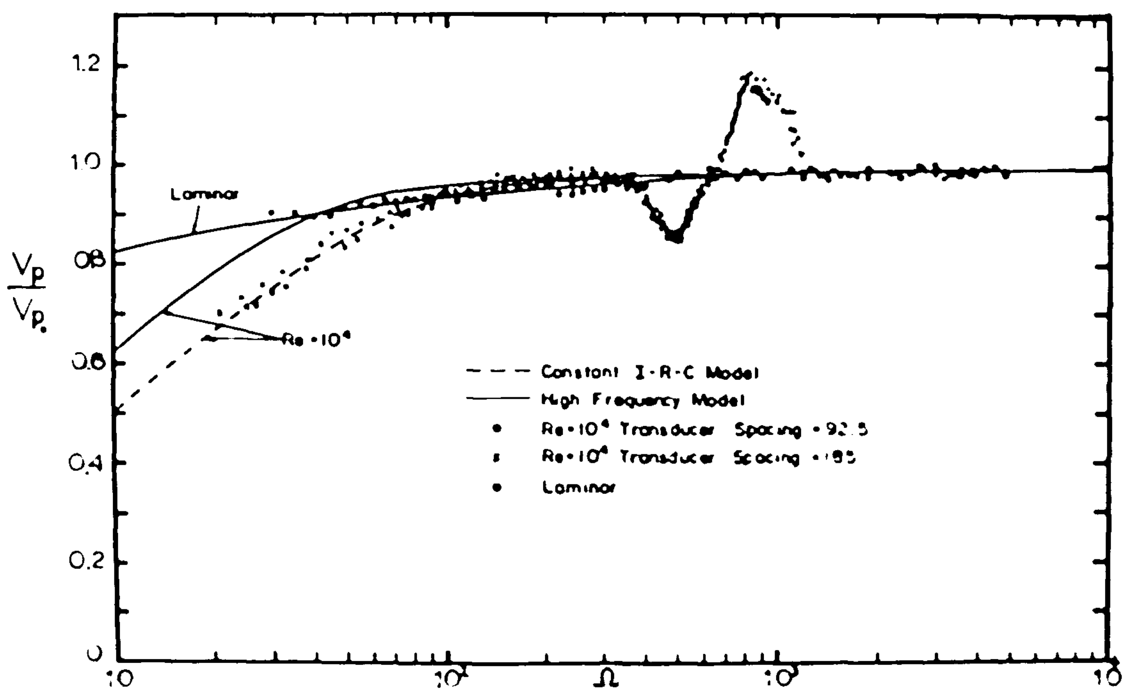

Laminar
Re = 10^4
Constant I·R·C Model
High Frequency Model
Re = 10^4 Transducer Spacing = 92.5
Re = 10^4 Transducer Spacing = 185
Laminar
$\frac{V_p}{V_{p_0}}$
Ω

Fig. 11

REFERENCES

1 Brown, F.T.,"Small-Amplitude Frequency Behavior of Fluid Lines with Turbulent Flow", Journal of Basic Engineering, Trans. ASME, Vol. 91, Series D, No. 4, Dec.,1969, pg 678-693.

2 Margolis, D.L.,"Measurement of the Propagation of Long-Wavelength Disturbances Through Turbulent Flow in Tubes", ASME Paper No. 75-FE-22, 1975.

3 Levine, H., "On the Radiation of Sound from an Unflanged Circular Pipe", Phys. Rev., Vol. 73, 1948, pg. 383-406.

4 Moody, L.F.,"Friction Factors for Pipe Flow", ASME Trans., Vol.66, No. 8, 1944, pg. 671.

5 Brater, E.F., Handbook of Hydralics, New York: McGraw Hill Book Co., 1976.

6 White, C.M.,"Streamline Flow Through Pipes", Proc. Roy. Soc., Vol. A 159, 1937, pg. 496.

7 Ito, H.,"Friction Factor in Turbulent Flow in Curved Pipes", Trans. ASME, Series D, Vol. 81, 1959, pg. 123.

VITA

Name: Robert Edwin Linney

Born: July 7, 1953

Place: Bridgeport, Connecticut

Parents: William Robert and Marion Judd Linney

Institutions Attended:	Andrew Warde High School, 1971
	Lehigh University, B.S. in M.E., 1976
	Lehigh University, M.S. in M.E., 1978